Title No. 113-S31

Testing of Reinforced Concrete Frames Extracted from a Building Damaged during the Canterbury Earthquakes

by Kevin Walsh, Richard Henry, Gye Simkin, Nicholas Brooke, Barry Davidson, and Jason Ingham

In the aftermath of the 2010-2011 Canterbury earthquakes in New Zealand, the residual capacity and reparability of damaged reinforced concrete (RC) structures was an issue pertinent to building owners, insurers, and structural engineers. Three precast RC moment-resisting frame specimens were extracted during the demolition of the Clarendon Tower in Christchurch after sustaining earthquake damage. These specimens were subjected to quasi-static cyclic testing as part of a research program to determine the reparability of the building. It was concluded that the precast RC frames were able to be repaired and retrofitted to an enhanced strength capacity with no observed reduction in displacement capacity, although the frames with "shear-ductile" detailing exhibited less displacement ductility capacity and energy dissipation capacity than the more conventionally detailed RC frames. Furthermore, the cyclic test results from the earthquake-damaged RC frames were used to verify the predicted inelastic demands applied to the specimens during the 2010-2011 Canterbury earthquakes.

Keywords: cyclic loading; ductility; earthquake; frames; precast concrete; reinforced concrete; shear-ductile.

INTRODUCTION

Clarendon Tower was a reinforced concrete (RC) office building located in Christchurch, New Zealand. The structure was designed to behave in a ductile manner based on the capacity design philosophy prescribed by contemporary New Zealand standards.[1,2] Inelastic demands were imposed on the building during the 2010-2011 Canterbury earthquakes, damaging the moment-resisting frames and potentially reducing their residual capacity. As a result, Clarendon Tower was deconstructed following the earthquake, affording the opportunity to extract three frame components from the building for structural testing. The extracted RC frames were repaired and subjected to simulated seismic loading in order to assess their residual capacity and reparability as well as to further understand the behavior of 1980s era precast concrete construction.

The goals of this investigation included determining the ductility that could be expected from the shear-ductile detailing used in several high-rise precast concrete buildings in New Zealand in the 1980s, verifying viable preventative or post-earthquake repair options for such shear-ductile reinforcement details, quantifying the level of performance enhancement from such repairs, and demonstrating that quasi-static testing of RC frame units extracted from damaged buildings could be used to verify the estimated demands imposed on the frames in preceding earthquakes.

RESEARCH SIGNIFICANCE

The research program described herein involved testing full-scale structural components extracted from a high-profile earthquake-damaged building. The test specimens were among the largest beam-column joint subassemblies that have been tested in New Zealand[3] and are thought to be among the largest components worldwide to be extracted from an actual building—in particular, from an earthquake-damaged building. The testing of these specimens provided direct evidence of the reparability of earthquake-damaged ductile structures as well as of the ductility capacity of RC buildings designed using 1980s design standards.

ORIGINAL CONSTRUCTION AND EARTHQUAKE DAMAGE

Clarendon Tower was an office building on the corner of Worcester Street and Oxford Terrace in Christchurch, New Zealand. The tower was designed in 1987 as a 20-story building,[4] including one basement level and two service levels at the top (refer to Fig. 1(a)). Clarendon Tower was constructed primarily of RC, using both precast and cast-in-place elements, as was common in New Zealand at the time of construction.[5-7] The structural system consisted of perimeter moment-resisting frames to provide lateral force resistance, and additional "gravity" frames located on two internal column lines to support the floors (Fig. 1(b)). The floors were constructed with 250 mm (9.8 in.) deep precast double-tees topped with 60 mm (2.4 in.) deep cast-in-place concrete reinforced with cold-drawn wire mesh. The precast double-tees spanned east-west bearing on the exterior beams on column lines B and L (refer to Fig. 1(b)) and the interior gravity beams on column lines E and I, with each floor span being approximately 7.7 m (25 ft 4 in.) long.

The north and south frames were designed with a "shear-ductile" diagonal bar detail (refer to Fig. 2(a)) that was intended to position the plastic hinge in the midspan portion of the beam to effectuate post-yield deformation in a shear mode, similar to the design philosophy commonly applied in coupled shear walls. This atypical configuration was necessary, as the short-span beams (approximately 2.1 m [6 ft 11 in.] clear span) and diagonal reinforcement details used in these north and south frames would have performed poorly if required to form flexural plastic hinges at the column faces. The east and west frames (refer to Fig. 2(b)) were more conventionally detailed for ductile behavior due to their relatively larger clear spans (approx-

ACI Structural Journal, V. 113, No. 2, March-April 2016.
MS No. S-2015-029.R2, doi: 10.14359/51688198, received June 17, 2015, and reviewed under Institute publication policies. Pertinent discussion including author's closure, if any, will be published ten months from this journal's date if the discussion is received within four months of the paper's print publication.

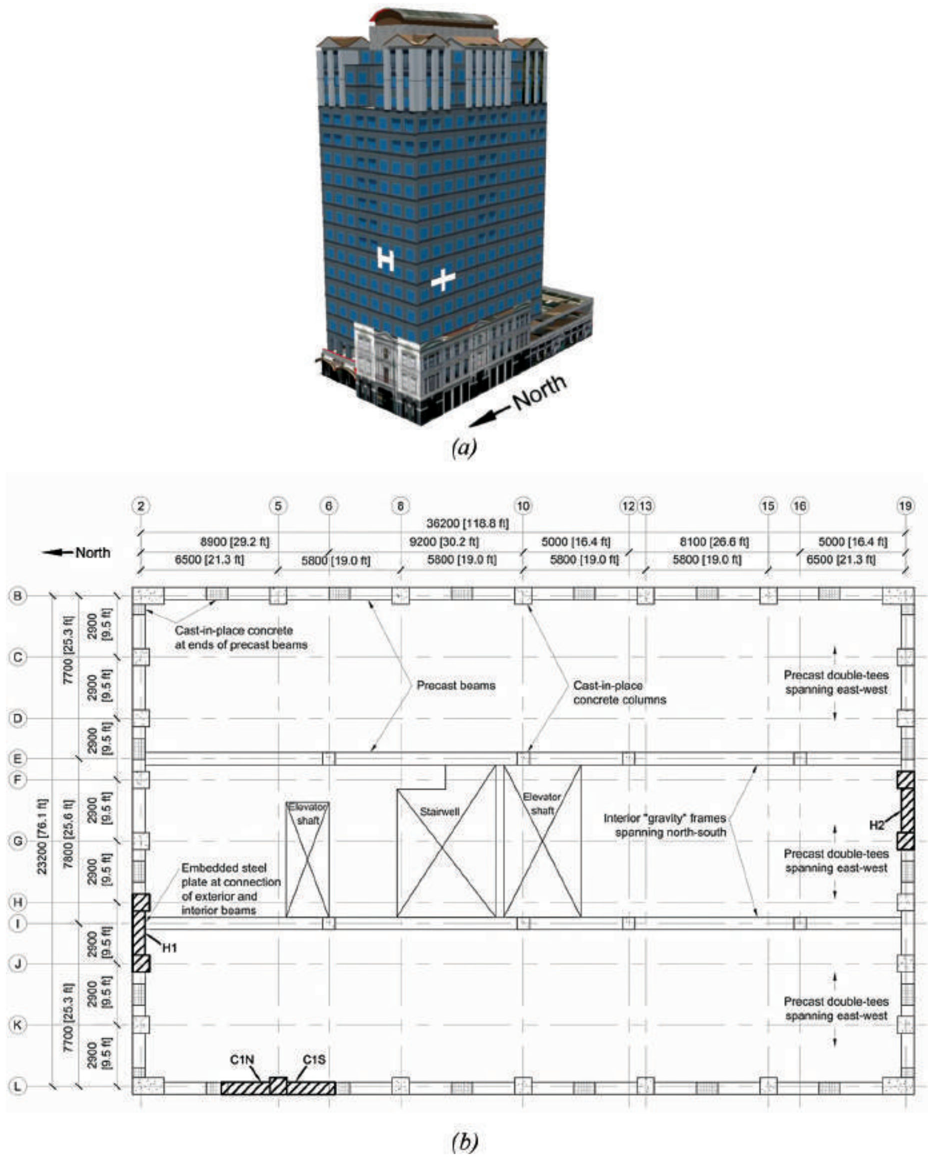

Fig. 1—Clarendon Tower frame construction indicating locations of extracted test specimens: (a) exterior isometric view[24]; and (b) typical tower plan. (Note: All units in mm unless noted otherwise; 1 mm = 0.0394 in.)

imately 5.0 m [16 ft 5 in.] clear span), with plastic hinges intended to develop in the beams at the column faces. Beams in the perimeter moment-resisting frames in the Clarendon Tower were constructed of precast concrete, and longitudinal reinforcement in the cast-in-place columns was passed through hollow ducts in the beams-column joints, which were then grouted. Cast-in-place concrete was used to stitch the beams together at various locations on the frames (refer to Fig. 1(b) and Fig. 2(b)).

The Canterbury region of New Zealand experienced an extended sequence of earthquakes in 2010 and 2011, with the two most prominent events occurring on 4 September 2010 (Darfield earthquake, M_W 7.1) and 22 February 2011 (Christchurch earthquake, M_W 6.2), subjecting Clarendon Tower to approximate peak ground accelerations (PGAs) of $0.22g$ and $0.43g$, respectively.[8] Clarendon Tower had been designed with a yield base shear coefficient of $0.048g$.[9] The performance of Clarendon Tower in the 2010-2011 Canterbury earthquakes, and the ensuing damage to the structure, has been reported extensively in other literature,[10-12] as was the temporary strengthening implemented to salvage the tenant fit-out and building materials during deconstruction in 2012 and early 2013.[9] The 2010-2011 Canterbury earthquakes caused moderate damage to the north and south moment-resisting frames of Clarendon Tower, and light damage to the east and west moment-resisting frames. Damage was most significant around the midheight levels where the column cross section reduced (refer to Fig. 2(a)). Damage was especially heavy at the north end of the building due to torsional behavior resulting from eccentric alignment of the tower relative to the podium as well as the placement of a heavy heritage façade along the street fronts on the first few stories (refer to Fig. 1(a)). Maximum displacement ductility demand at Level 8 was estimated to be $\mu = 4.0$ in the north frame and $\mu = 2.0$ or less in the other frames, based on computational analysis.[11]

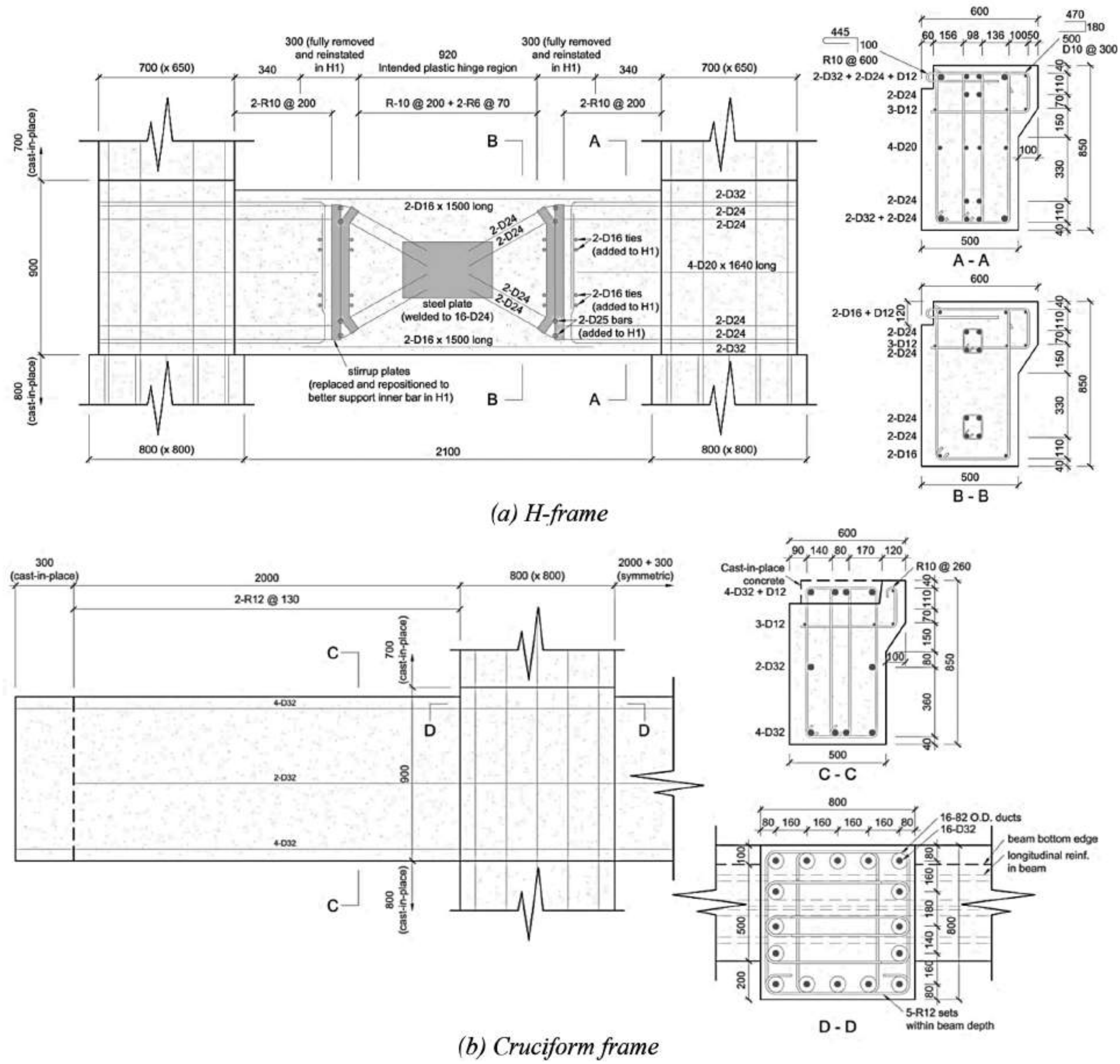

Fig. 2—Beam geometry and reinforcement detailing. (Note: Column reinforcement and some secondary reinforcement not shown for simplicity; D is deformed bar; R is round bar; all units in mm; 1 mm = 0.0394 in.)

EXPERIMENTAL INVESTIGATION

Test specimens

A total of three frame specimens, consisting of four separate beams total, were extracted from Clarendon Tower and tested in Auckland. The test beam types and locations within the building are summarized in Table 1 and illustrated in Fig. 1 and 2. The test frames are referenced by the general form in which they were extracted from the building—"H" for H-frames composed of two columns at either end of a short beam, and "C" for cruciform frames composed of a single column with longer beams on either side. Frames were extracted in these forms to ensure that the intended plastic hinge regions of the beams could be tested with appropriate boundary conditions. All test specimens were extracted from the more highly damaged midheight portion of the building (refer to Fig. 1(a)). As shown in Fig. 2, all test specimens represented a single-story unit of the respective frames, but due to transportation limitations, the heights of the columns were limited to 2400 mm (7 ft 10.4 in.). Steel extensions were attached to the ends of the columns during testing so that the total column length was equal to the story height of Clarendon Tower, which was approximately 3400 mm (11 ft 1.9 in.) at the levels from which the test frames were extracted.

Damage to the H-frame specimens from the 2010-2011 Canterbury earthquakes can be seen in Fig. 3. Contrary to the original design intent of the "shear-ductile" link, but consistent with the results of previous experimental testing on similarly detailed specimens[13] and strut-and-tie analysis,[10,11] both H-frame specimens sustained the most extensive damage approximately 500 mm (19.7 in.) from the column face, near the locations where the reinforcement was bent to form the diagonal (indicated in Fig. 2(a) by the position of the steel stirrup plates). Residual crack widths at these locations were as large as 7 and 5 mm (0.28 and 0.20 in.) in Specimens H1

Table 1—Summary of identification and condition of specimens

Test ID	Geometry and detailing	Building location (refer to Fig. 1)	Damage and repairs
H1	Fig. 2(a)	Underside of Floor 8 along Column Line 2 (north elevation) between Column Lines H and J	More heavily damaged; repaired and retrofitted with new reinforcement and high-strength concrete
H2	Fig. 2(a)	Underside of Floor 8 along Column Line 19 (south elevation) between Column Lines F and G	Lightly damaged; repaired with crack injection
C1N	Fig. 2(b)	Underside of Floor 7 along Column Line L (west elevation) from Column Line 5 toward 2	Lightly damaged; crack injection repairs were begun but not completed following the Sept. 2010 earthquake
C1S	Fig. 2(b)	Underside of Floor 7 along Column Line L (west elevation) from Column Line 5 toward 8	

(a) Heavier cracking on specimen H1 *(b) Lighter cracking on specimen H2*

Fig. 3—Post-earthquake damage to H-frame specimens with crack widths indicated. (Note: All units in mm; 1 mm = 0.0394 in.)

and H2, respectively, as shown in Fig. 3. Multiple large cracks in Specimen H1 protruded from the location of an embedded steel plate (visible to the right in Fig. 3(a)), which was included in the unit to connect the perimeter frame to the interior gravity frame (Fig. 1(b)). Diagonal cracks in the beam-column joint region of both H-frame specimens were typically less than 0.3 mm (0.01 in.) wide and only superficial cracking was observed in the columns.

Specimen H1 was taken from the most damaged region of the exterior building frame—the north side of the eighth floor—where in-place repair and retrofit of the beams would likely have been required had the building not been deconstructed. To verify whether Clarendon Tower could have been repaired to a state of structural integrity equaling or exceeding its capacity prior to the earthquakes, repairs were commissioned for Test Specimen H1 in the manner in which they would have been proposed on the in-place structure. Specimen H1 was repaired and retrofitted based on a technique previously validated in New Zealand[13] and consisted of the following steps:

1. Concrete surrounding the steel stirrup plates was removed using hydrodemolition to avoid damaging the reinforcing steel (refer to Fig. 2(a) and Fig. 4(a));

2. Additional transverse reinforcement consisting of D25 bars (where "D" represents "deformed" bar, and the diameter is 25 mm [0.98 in.]) was placed at the inside of each bend of the original D24 (0.94 in.) diagonal reinforcement bars to improve bearing strength at these locations (refer to Fig. 2(a) and Fig. 4(b));

3. The steel stirrup plates shown were replaced and repositioned so that bearing stresses were more evenly distributed between inner and outer bent D24 (0.94 in.) bars (refer to Fig. 2(a) and Fig. 4(b));

4. Transverse hoop ties consisting of D16 (0.63 in.) bars were added around the vertical legs of the hooks formed where the D32 (1.26 in.) reinforcement bars terminated at the interface with the diagonal reinforcement detail (refer to Fig. 2(a) and Fig. 4(b)); and

5. Flowable concrete with a nominal compressive strength of 60 MPa (8.7 ksi) was used to reinstate the concrete removed via hydrodemolition.

Specimen H2 was taken from the less damaged south frame where it experienced minor to moderate cracking, as shown in Fig. 3(b). Epoxy injection was used to repair the H2 specimen, as shown in Fig. 4(c), and no further retrofit enhancements were used. Likewise, Specimen C1 (composed of Beams C1N and C1S denoting relative orientations "north" and "south" on the building per Fig. 1(b)) sustained only minor to moderate cracking during the earthquakes, as shown in Fig. 5. Specimen C1 had begun to be prepared for crack injection after the September 2010 earthquake, as shown in Fig. 5(a), but repairs were not completed prior to the February 2011 earthquake and subsequent demolition of the building. Due to the preparation for repairs, the widths of larger residual cracks in the beam ends near the joint could not be measured reliably. Other residual crack widths in the beams and beam-column joint region were generally less than 0.3 mm (0.01 in.). As with the H-frame specimens, no measureable cracking was observed in the column outside the joint region. As the damage to the cruciform beams was not anticipated to affect their structural performance, Beams C1N and C1S did not receive any further repair prior to testing, such that these specimens were tested in their post-earthquake-damage state. Repair of these frames in-place would only have been required for reasons of cosmetics and durability.

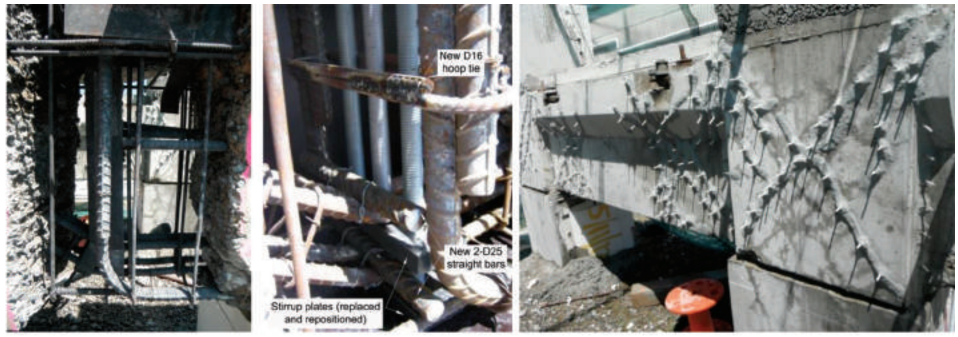

(a) Heavier repairs on specimen H1 (hydraulic demolition and reinstatement) *(b) Retrofit of specimen H1* *(c) Lighter repairs (crack injection) on specimen H2*

Fig. 4—Repair of earthquake damage to H-frame specimens.

(a) Residual damage and uncompleted repairs on the interior (east) face of the south beam (C1S) *(b) Residual cracks marked on the exterior (west) face*

Fig. 5—Post-earthquake damage to cruciform frame specimen.

Test setup

The test specimens were placed into a custom-made self-reacting steel frame that could be configured to accommodate both the H- and C-frame specimens, as shown in Fig. 6. The columns of the test specimens were extended to full-story height and attached to the steel reaction frame by heavy steel shoes placed at the column ends. These shoes were clamped to the column ends by way of six external post-tensioned steel rods on each column, with the prestress in each column approximately equal to the expected building gravity load of 2300 kN (517 kip).

The H-frame test setup shown in Fig. 6(a) and Fig. 7(a) comprised the specimen hanging from a pin restraint at one column and a link restraint at the other column that allowed for axial elongation of the beam plastic hinges during testing. Simulated earthquake loading was applied to the test specimens by double-acting hydraulic jacks. For the H-frame specimens, the primary jacks were placed at the bottom of the two columns to apply lateral drift to the frame, with a third compensating jack at the top link connection that was adjusted as frame elongation occurred. Positive drift was defined as displacement of the bottom of the columns toward the west within the Auckland test site.

The cruciform test setup shown in Fig. 6(b) and Fig. 7(b) comprised the specimen hanging from a pin restraint at the top of the column with a jack attached to the bottom of the column to impose a lateral drift on the frame. Due to limitations on the forces that could be reliably applied with the test equipment, the north and south beams (C1N and C1S, respectively) were tested independently. The end of the beam being tested was attached to a link connection that restrained the beam end against vertical displacement (but permitted end rotation and longitudinal translation), and the end of the beam not being tested was left free to rotate. Positive drift for the beams was defined as corresponding with the top of the beams being in tension. Note that the results of previous experimental testing on similarly detailed cruciform specimens in which both beams were restrained simultaneously[13] indicated that the column and beam-column joint (refer to Fig. 2(b)) were very stiff relative to the beams and contributed relatively little to the ductile deformation mechanisms of the frame. These experimental findings were consistent with the design intentions for contemporary beam-column joints[1,5-7] to both ensure the appropriate development length of reinforcement through the beam-column joints so as to limit bond deterioration due to cyclic loads on beams on opposite sides of the joint region, and to size and detail the

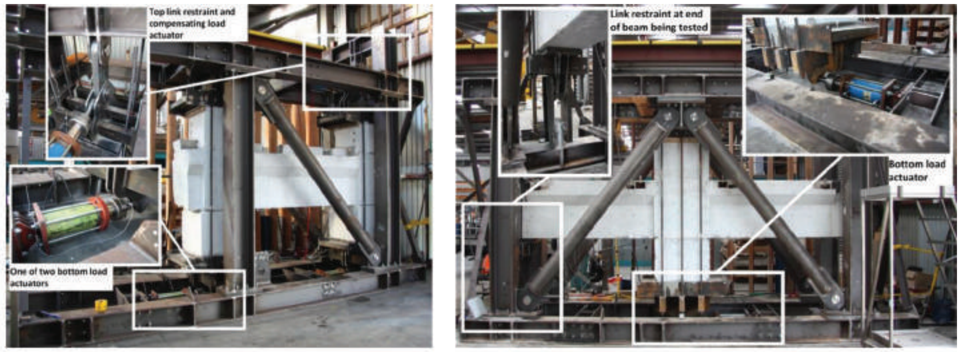

(a) H-frame specimen (b) Cruciform specimen (C1N on left and C1S on right)

Fig. 6—Test setup with steel reaction frame and RC test specimens (left is west within the Auckland test site); inserted photos of load actuators and link restraints.

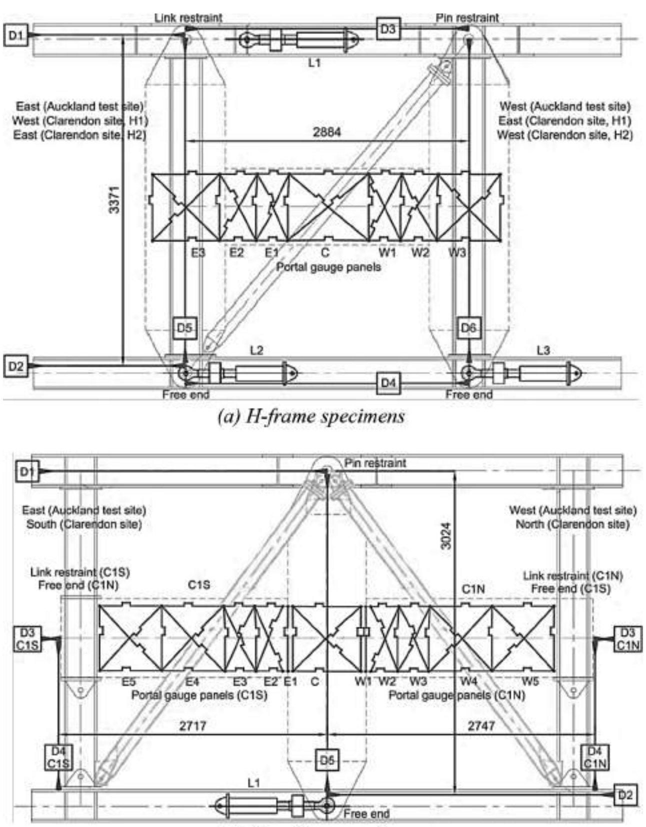

Fig. 7—Basic instrumentation plans and restraint conditions for test specimens. (Note: L is load cell; D is displacement gauge; all units in mm; 1 mm = 0.0394 in.)

columns to ensure their higher stiffness and strength relative to the beams. Finally, note that no explicit out-of-plane restraints were present in the reaction frame, although the pin restraints, link restraints, and hydraulic jacks used in both test arrangements (H-frame and cruciform) permitted only uniaxial movement at their respective locations.

Instrumentation plans

The frames were instrumented with a range of different gauges to measure the global response of the test specimens as well as the local response of the beams and beam-column joints during testing. The general instrumentation arrangement used for the H-frame test specimens is shown in Fig. 7(a). A total of three load cells (L) and 43 displacement gauges (D) were used in the testing of the H-frame specimens. In addition to measuring the total load and drift demands applied to each specimen, displacement gauges were also placed across the beam, as shown in Fig. 7(a), to measure local deformations within the beam element. These displacement gauges were attached to rods that were epoxied into holes drilled in the side of the beam. The net lateral interstory drift of the H-frame specimens was calculated from both horizontal and vertical displacements measured at the ends of the columns. The total story shear was determined by summing the reactions L2 and L3 at the bottom of the columns (whereas L1 was simply used to maintain equilibrium as the beam elongated).

The instrumentation plans used for the two cruciform beam test specimens are shown in Fig. 7(b). One load cell and 35 displacement gauges were used in the testing of each cruciform beam specimen. As with the H-frame specimens, displacement gauges were also placed across the cruciform beams to measure local deformations within the beams. The net lateral interstory drift of the cruciform beam specimens was calculated from both horizontal and vertical displacements at the ends of the column and beam.

Loading sequence

Testing of all frames was performed in accordance with the general loading protocol commonly used in New Zealand[14] and was consistent with international standards,[15] using pairs of cycles at progressively increasing magnitudes of net interstory drift. Loading cycles were continued until the displacement limits of the test equipment were reached. These limits resulted in displacing the H-frame units to approximately 2.0% net interstory drift and the cruciform units to approximately 4.0% net interstory drift, which exceeded the respective drifts expected to occur in Clarendon Tower during a design basis earthquake (DBE) based on ultimate limit state (ULS) criteria, which correspond to the life safety (LS) performance level criteria considered in ASCE 41.[16] Furthermore, the maximum test drift demands exceeded the drift demands estimated to have been imposed on the respective frame components during the 2011 Christchurch earthquake. The loading protocol for the H-frame specimens consisted of two cycles each at approximate drift demands of ±0.2%, 0.4%, 1.2%, and 2.0%. The second drift limit (that is, 0.4%) was determined prior to testing to have approximately equaled the yield drift of similar H-frame specimens previously tested in New Zealand.[13,17] The control sequence for the cruciform specimens consisted of two cycles each at approximate drift demands of ±0.5%, 1.0%, 2.0%, 3.0%, and 4.0%. The first drift limit of 0.5% was estimated to represent the yield drift of the cruciform frames based on a simplified, empirically-based procedure.[18,19] C1N was only tested to one complete cycle of drifts at ±4.0% due to limitations in the test frame, whereas C1S was tested to two complete cycles of drifts at ±4.0%.

Material properties

Eight cylindrical concrete core samples each approximately 100 mm in diameter and 200 mm in length (3.94 x 7.87 in.) were drilled from undamaged regions of the test specimens following the cyclic loading tests. These cored samples were tested to determine the compressive strength, elastic modulus, and splitting tensile strength of the precast concrete used in these frame specimens. Laboratory testing was performed in accordance with New Zealand Standards,[20] and the compressive tests were consistent with international standards.[21] The compression test results were based on five core samples in which two cores were taken from each of the H-frame specimens and one core was taken from the cruciform frame specimen. The mean maximum cylinder compressive strength and mean elastic modulus were 35.3 MPa and 25.6 GPa (5.1 and 3713 ksi), respectively. The splitting tensile test results were based on three core samples in which one core was taken from each of the three test frame specimens. The mean splitting tensile strength was 4.2 MPa (0.6 ksi). Smooth alluvial coarse aggregate common in Canterbury concrete construction was visibly prominent in the cored samples.

The primary longitudinal steel reinforcement in the test frames was designated on the original plans[4] as having minimum yield strengths of 276 and 380 MPa (40 and 55 ksi) in the beams and columns, respectively. It was impractical to remove and test any steel reinforcement samples from the test frames due to the specimens having been previously damaged in the earthquakes and the subsequent likelihood that the primary longitudinal reinforcing steel had already yielded. Furthermore, contemporary steel reinforcement material properties are considered extensively in other literature, with particular consideration given to the effects of strain aging[17,22] and low-cycle fatigue.[23] For purposes of determining the expected performance of the test specimens, the steel reinforcement in all of the test beams was assumed to have an actual yield strength of 321 MPa (47 ksi), based on previous tests of contemporary steel in New Zealand.[13]

EXPERIMENTAL RESULTS

H-frame general observations

Images of damage state conditions at progressively larger drift cycles for Specimens H1 and H2 are shown in Fig. 8. At low drift levels, flexural cracks formed near the beam ends and propagated at approximately 45 degrees through the web region of the beam due to the high shear demand in the short span. Flexural cracks at the bottom edge of the beams were reasonably well distributed, approximately corresponding to the stirrup spacing. Flexural cracks at the top edge of the beams were less uniformly distributed and concentrated at two to three wider cracks due to the presence of embedded steel plates and anchors associated with the exterior cladding. After drift demands of approximately ±1.2% were reached, wide cracks started to open up in both H-frame specimens approximately 500 mm (19.7 in.) from the beam ends at the location where the "bend" of the diagonal reinforcement occurred (refer to Fig. 2(a)). During subsequent cycles, the damage was concentrated at these locations, which is consistent with the locations on the beams that were most damaged occurred during the 2010-2011 earthquakes (refer to Fig. 3). The locations of damage concentration were bounded by displacement gauge panels E1 and W1 (refer to Fig. 8). The cracks at these locations reached widths exceeding 8 mm (0.31 in.) at maximum drifts of approximately ±2.0%, and a shear-sliding mechanism became visibly prominent. In the case of the H1 specimen, damage caused by shear-sliding was especially and narrowly concentrated within the region of the beam bounded by panel W1, with significant spalling occurring during cycles to ±2.1% drift. In the case of the H2 specimen, damage was more evenly distributed between both ends of the beam, resulting in more symmetrical spalling and loss of concrete cross-section within gauge panels E1 and W1.

Despite the design intent for the plastic hinges to be concentrated at the "shear-ductile" link with diagonal reinforcement at the central panel region (C), only relatively minor cracking occurred in this region for both H-frame specimens. The lack of observed damage to the central "shear-ductile" link was consistent with the design deficiency that was discovered during previous testing of this type of detail,[13] and it appeared that the repair to the H1 test specimen did not prevent the damage from concentrating at the location of the bar bends. No primary longitudinal steel reinforcing bars were observed to have ruptured during the testing of either H-frame specimen, although some primary longitudinal bars were deformed vertically (that is, transversely to their originally longitudinal axes) during the development of the shear-sliding mechanisms.

H-frame tests—global response

The global lateral force-drift response and calculated hysteretic energy dissipation of the two H-frame specimens are compared in Fig. 9(a) and Fig. 9(b), respectively. The repaired and retrofitted H1 specimen exhibited a higher strength (Fig. 9(a)) and greater energy dissipation at large drifts (Fig. 9(b)) when compared to the H2 specimen, which was repaired only with epoxy injection and more closely represented the as-built condition of the H-frame components prior to the earthquakes. The response of both H-frame specimens was not stable, and softened in terms of strength and energy dissipation capacity at subsequent cycles to equivalent drift levels. As shown in Fig. 9(a), the strength

Fig. 8—Damage state conditions at progressively higher drift levels for H1 (left, repaired, and retrofitted) and H2 (right, repaired only) specimens with approximate portal gauge panel regions indicated (gauges physically located on opposite side of specimens).

of the H1 test specimen decreased by approximately 10% during the negative portion of the first cycle of loading to a drift of –2.1% and by approximately 20% for both loading directions during the second cycle to a drift of ±2.1%. The strength of the H2 test specimen decreased by approximately 15% during the second cycle of loading to a drift of ±1.3%, sustained this reduced load capacity during the first cycle to a drift of ±2.1%, and then decreased further to approximately 20% below the initial peak strength during the second cycle to a drift of ±2.1%. Testing of each unit was concluded after the completion of two reversed loading cycles to an approximate drift of ±2.1%, approximately equivalent to a displacement ductility μ = 5.2. As shown in Fig. 9(a), pinching occurred in the hysteresis loops of both H-frame specimens (but especially the non-retrofitted H2 specimen) due to the prominence of shear-sliding mechanisms at higher drifts, limiting the energy dissipation capacity of the H-frames at higher drift levels. The pinching in the hysteresis response was more evident for the H2 specimen, with the H1 specimen displaying somewhat greater energy dissipation.

Restrepo[13,17] used the geometry and detailing of the H-frame specimens extracted from Clarendon Tower as the prototype for precast shear-ductile beam specimens tested previously. The anticipated and measured yield drift of 0.4% for the Clarendon H-frame specimens was approximately equal to that of the Restrepo units. The anticipated interstory shear yield strength of the H2 (repaired only) specimen was 496 kN (112 kip) using Restrepo's recommended analytical procedure assuming initial yield in the diagonal shear reinforcement,[17] and is shown superimposed on the measured

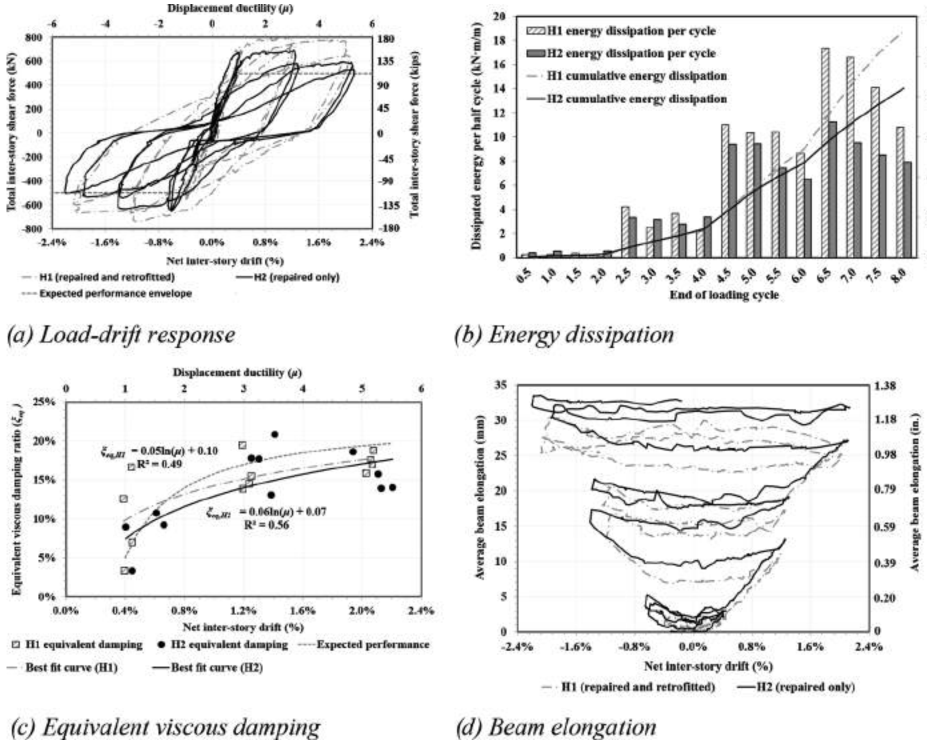

(a) Load-drift response

(b) Energy dissipation

(c) Equivalent viscous damping

(d) Beam elongation

Fig. 9—Comparison of global performance of the two H-frame test specimens. (Note: 1 kN = 0.225 kip.)

responses in Fig. 9(a). The strength of both H-frame specimens measured during testing exceeded the calculated yield strength. This difference was attributed to the effects of strain aging in the steel reinforcement, which likely resulted from the preceding earthquake demands, which were especially high on the north and south frames from which the tested H-frame specimens were extracted. It should also be noted that the frames would potentially have had greater capacities within the building due to the contribution of the floor diaphragm to the flexural strength.

The energy dissipation per half cycle (Fig. 9(b)) was determined from the corresponding hysteresis area (Fig. 9(a)). The energy dissipation was then converted to an equivalent viscous damping per half cycle, with the results plotted in Fig. 9(c) for Test Specimens H1 and H2. Retrofitted specimen H1 exhibited slightly higher equivalent viscous damping at lower drifts than Specimen H2, corresponding to larger hysteresis loops at lower drifts (Fig. 9(a)). However, the equivalent damping for the H1 and H2 specimens was similar at higher drifts. The expected equivalent damping performance graphed in Fig. 9(c) was determined using the method proposed by Priestley et al.[19] for more typically detailed RC frames. Note that Specimens H1 and H2 had equivalent viscous damping capacities slightly less than typical RC frames at high displacement ductility demands, most likely due to the presence of a shear mechanism with pinched hysteresis behavior as opposed to a more desirable and conventional flexural inelastic mechanism.

Average axial beam elongation measured at the center of the beam section is plotted in Fig. 9(d) for Test Specimens H1 and H2. Maximum elongation for both specimens at maximum drifts exceeded 30 mm (1.18 in.), which represented approximately 3.5% of the beam depth and a 1.4% increase in beam length. It appeared that the top link restraint (refer to Fig. 6(a)) did not limit the maximum elongations measured in the H-frame specimens. The elongation for both H-frame beams at inelastic drift levels was effectively irrecoverable and progressively increased at subsequent cycles of equivalent drift levels. The non-retrofitted specimen, H2, elongated slightly further than the retrofitted specimen, H1, at similar drift levels. Frame elongation in the building during the earthquake was partially restrained by the presence of the adjacent floor diaphragm components. The total residual elongation of the north frame in the east-west direction of the building was measured at a maximum of 50 mm (1.97 in.) over eight bays, or 6.25 mm (0.25 in.) per bay on average, despite the estimated maximum drift demands in the east-west direction imposed by the 2011 Christchurch earthquake on the north frame being as high as 2.8%.[10,11] Hence, the maximum beam elongations measured during testing and indicated in Fig. 9(d) may not be indicative of the expected behavior of these frames in the building with the floor diaphragm in place adjacent to the beams. Note, however, that the considered computational analysis[10,11] did not include the potentially stiffening effects of the precast concrete cladding on the building performance, and so the ductility demands determined in the computational model may have been overestimated.

H-frame tests—local response

The contributions of local deformation components to the total interstory drifts of the H-frame specimens (measured using the gauge setup shown in Fig. 7(a)) are plotted in Fig. 10. Note firstly that flexural mechanisms, particularly at the ends of the beams by the columns (Panels E2 and W2), contributed more to interstory lateral displacement at lower drifts, and that the contribution from shear mechanisms became more prominent at higher drifts. On both

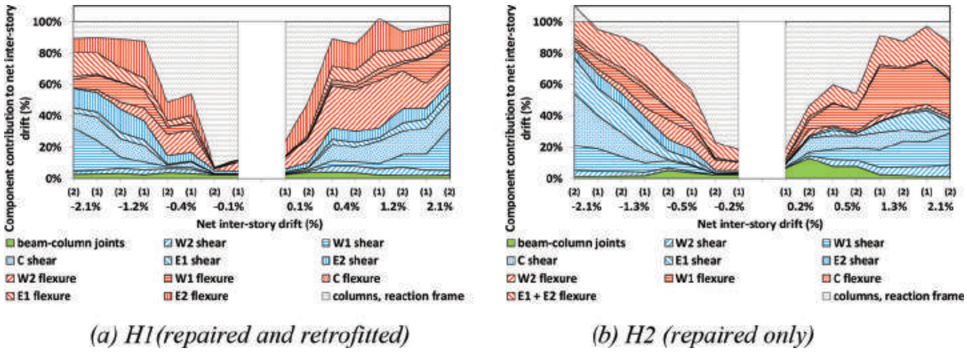

Fig. 10—Component contributions to interstory drifts of H-frame specimens.

H-frame specimens at high drift demands, the center panel region (C) contributed less to total frame deformation than intended by its shear-ductile design,[13] and the beam end regions (E2 and W2) contributed less to total frame deformation than in traditional moment-resisting frame design.[19] The locations of prominent deformation mechanisms at high drifts occurred within gauge panel regions, E1 and W1, on both H-frame specimens. The more symmetric distribution of shear deformation in Panels E1 and W1 in Specimen H2 at high drifts (refer to Fig. 10(b)) as compared to the greater concentration of shear deformation in Panel W1 in Specimen H1 (Fig. 10(a)) was likely due to the presence of an embedded steel plate in the W1 region of Specimen H1 (Fig. 1(b) and Fig. 3(a)). Measured deformations within the beam-column joint regions contributed relatively little to the total interstory drifts of both H-frame specimens.

The localized regions of measured deformation concentration in the H-frame specimens corresponded with areas of visually observed damage concentration from the earthquakes (refer to Fig. 3) and from testing (Fig. 8). Furthermore, the measured deformation mechanisms plotted in Fig. 10 were consistent with the expected deformation mechanisms determined from the strut-and-tie analysis performed after the earthquakes,[10,11] which predicted that strain concentration would occur in the top and bottom D24 reinforcing bars (Fig. 2(a)) near to but on the column sides of the stirrup plates due to bond action transferring the forces in these bars to the D32 reinforcing bars over a short distance. Furthermore, the bend in the D24 bars inside the stirrup plates may have mechanically strain hardened the reinforcement at that location, further increasing strain concentration in the bars just outside the stirrup plates[10] as well as creating an outward "bursting" force[13] effectuating a shear-sliding mechanism in the E1 and W1 panel regions. The retrofit implemented in Specimen H1 (refer to Fig. 4(b)) improved slightly the measured deformation mechanisms. Note that retrofitted specimen, H1, had a maximum measured shear contribution to interstory drift in Panel E1 of 5% (Fig. 10(a)), while non-retrofitted specimen, H2, had a maximum measured shear contribution in Panel E1 of 23% (refer to Fig. 10(b)), with Panel W1 being disregarded in this comparison due to the embedded plate at that location in Specimen H1. However, the retrofit did not appear to improve the measured shear contribution to interstory drift in Panel C at high drifts (refer to Fig. 10). Hence, the retrofit implemented in Specimen H1 strengthened the shear-sliding mechanism by improving the bearing stress distribution of the bent D24 bars but did not have a significant effect on altering the primary damage mechanism.

Cruciform tests—general observations

Images of damage state conditions at progressively larger drift cycles of Specimens C1N and C1S are shown in Fig. 11. The damage pattern was consistent for the two cruciform beams, as would be expected due to their similar detailing. As with the H-frame beams, flexural cracks formed at low drifts with relatively regular spacing corresponding to the stirrup spacing at the bottom of the beams. Initial flexural cracks at the top of the beams were less uniformly distributed and corresponded with areas stiffened by embedded plates and anchors originally installed for connecting exterior cladding to the frame (refer to Fig. 5(b)). Damage concentration in the intended plastic hinge regions[19] at the beam ends near the column (E2 and W2 in Fig. 11) became prominent at drifts of approximately ±2.0%, at which point primary flexural cracks in these regions opened to widths exceeding 8 mm (0.31 in.). Moderate spalling in the beam end regions, primarily due to concrete crushing, occurred at drift levels of approximately ± 3.0%. More significant spalling occurred at drift levels of approximately ±4.0%.

The greater extent of damage in C1S at the conclusion of testing (observable in Fig. 11) was due to this unit having been tested to two cycles of drifts at ±4.0% as compared to Beam C1N, which was tested to only one cycle of drifts at ±4.0%. As a result, the more prominent buckling of the primary longitudinal reinforcement observed in Specimen C1S was likely associated with complete spalling of the cover concrete around almost the entire circumference of the beam in the end region (E2). At the end of the test, it was observed that one of the top longitudinal reinforcing bars of both beams (C1N and C1S) had been completely cut through approximately 100 mm (3.94 in.) from the face of the column during the process of the specimen's removal from Clarendon Tower, resulting in slightly greater crack openings at the top of the beams as compared to the underside of the beams at similar drifts. Aside from the saw-cut reinforcement, no primary longitudinal steel reinforcing bars were observed to have ruptured during the testing of either cruciform beam specimen.

Cruciform tests—global response

The global lateral force-drift hysteretic behavior of the two cruciform beam specimens is compared in Fig. 12(a). C1N and C1S consistently exhibited behavior similar with one another, as would be expected due to their similar detailing and residual damage levels. The strength of both cruciform beams increased through all positive drift cycles up to the first positive drift cycle of approximately +4.0% (noting that Beam C1N was only subjected to one cycle at this drift demand). The strength of C1N decreased approximately 20% during its second cycle to a drift of –3.0%, and approximately 50% below the initial peak strength during its first and only cycle to a drift of –4.0%. The strength of C1S decreased approximately 15% during the first cycle to a drift of –4.0% and approximately 50% below the initial peak during the second cycle to a drift of –4.0%. The strength reductions measured while testing the cruciform specimens may be attributed to the crushing of weaker topping concrete at the tops of the beams as well as the observable buckling of longitudinal bars near the beam interface with the column (Panels W2 and E2 for C1N and C1S, respectively; refer to Fig. 11). When compared to the H-frame specimens, the more traditionally detailed cruciform beam specimens exhibited less hysteretic pinching and greater drift ductility.

The measured yield drift of the Clarendon cruciform beam specimens of 0.65% was slightly higher than the anticipated value of 0.5% predicted using a simplified, empirically-based procedure,[18,19] but well within the typical scatter of such comparisons.[3] The anticipated interstory shear strength of the cruciform frames was 347 kN (78 kip) based on an ultimate flexural strength of 1050 kN-m (774 kip-ft), as determined for the beam by a simple cross-sectional analysis. The expected strength closely matched the measured test strength (as shown in Fig. 12(a)), which indicated that no significant strength enhancement occurred due to strain aging following the 2010-2011 earthquakes.

The two cruciform beams exhibited similar cumulative dissipated energy capacities (refer to Fig. 12(b)), with the slight difference in measured dissipated energy likely being the result of slightly different applied drift demands. Softening at subsequent cycles of low and intermediate equivalent drift levels was less pronounced for the cruciform beams than for the H-frame beams. Note, however, the significant drop in energy dissipation capacity for C1S at the end of half cycles 9.5 and 10.0 in Fig. 12(b). The energy dissipation per half cycle was converted to equivalent viscous damping, with the results plotted in Fig. 12(c) for Test Specimens C1N and C1S. The expected equivalent damping performance determined using the method proposed by Priestley et al.[19] for conventionally detailed RC frames corresponded closely with the equivalent damping ratios measured from the tested Clarendon cruciform beams.

The measured axial elongations of the cruciform beams at varying drift demands are shown in Fig. 12(d). The beam end link restraint (Fig. 6(b)) appeared to limit the cruciform beam elongation at high negative drifts by imposing an offsetting compressive load onto the beam section. Note that the tested length of Beam C1N was slightly longer than the tested length of Beam C1S (refer to Fig. 7(b)), likely resulting in the beam end link restraint being especially restraining in regard to the elongation of Beam C1S at higher drifts. As with the H-frame specimens, the maximum beam elongations shown in Fig. 12(d) may not be indicative of the expected behavior of these frames in the building due to the restraining effects of the adjacent floor diaphragm in the building.

Cruciform tests—local response

The contributions of local deformation components to the total interstory drifts of the cruciform frames (measured using the gauge setup shown in Fig. 7(b)) are plotted in Fig. 13. First, note that the contribution from flexural mechanisms was far more prominent at all drift levels for the cruciform beams as compared to the H-frame specimens, particularly within the beam end regions by the columns (Panels W2 and E2 in Beams C1N and C1S, respectively). Deformations measured in panel regions W1, W5, E1, and E5 represented insignificant proportions of the total interstory deformation and, therefore, were combined in Fig. 13 with other small deformation components and those that were not able to be accurately measured (notably, the contribution of deformations to the net interstory drift within the cruciform column). Note that these other contributions to interstory drift were especially prominent at high negative drift levels (likely due to restraint from the beam end link), and likely offset contributions to net drift from the primary panel regions at high drift levels. The localized regions of measured deformation concentration corresponded with visible areas of damage concentration both from the earthquake (refer to Fig. 5) and from testing (Fig. 11), and were also consistent with the expected deformation mechanisms in traditional moment-resisting frame design.[19] As with the H-frame specimens, measured deformations within the beam-column joint regions of the cruciform beams contributed very little to total interstory drifts of the frames.

COMPARISON OF PREDICTIONS AND EXPERIMENTAL RESULTS

For the frame specimens tested in this program, comparisons of the analytical predictions, visual observations, and experimental measurements are summarized as follows:

1. Maximum estimated drift demands imposed by the 2011 Christchurch earthquake on Levels 5 to 10 of Clarendon Tower were approximately 1.3% for deformations in the north-south direction and 1.3% to 2.8% for deformations in the east-west direction, with the northern perimeter frame expected to experience more deformation than the southern frame due to torsional effects.[10,11] These estimated drift demands corresponded well with residual crack widths and locations observed and recorded prior to testing (refer to Fig. 3 and 5) and at similar drift levels during testing (Fig. 8 and 11);

2. The anticipated interstory yield drift and strength of the H2 (repaired only) specimen were 0.4% and 496 kN (112 kip), respectively, using Restrepo's[13,17] test results and recommended analytical procedure, respectively. A nearly equivalent yield drift to the prediction was measured during testing for both H-frame units, but the measured strength

Fig. 11—Damage state conditions at progressively higher drift levels for C1N (left) and C1S (right) beam specimens with approximate portal gauge panel regions indicated (gauges physically located on opposite side of specimens).

was approximately 60% and 40% higher than predicted for specimens H1 and H2, respectively (refer to Fig. 9(a)), likely due to strain aging of the longitudinal reinforcement. The anticipated interstory shear yield drift and strength of the cruciform beams was 0.5% and 347 kN (78 kip), respectively, using a simplified, empirically based procedure[18,19] and traditional RC beam cross-sectional analytical procedures, respectively. A slightly higher, but similar, yield drift

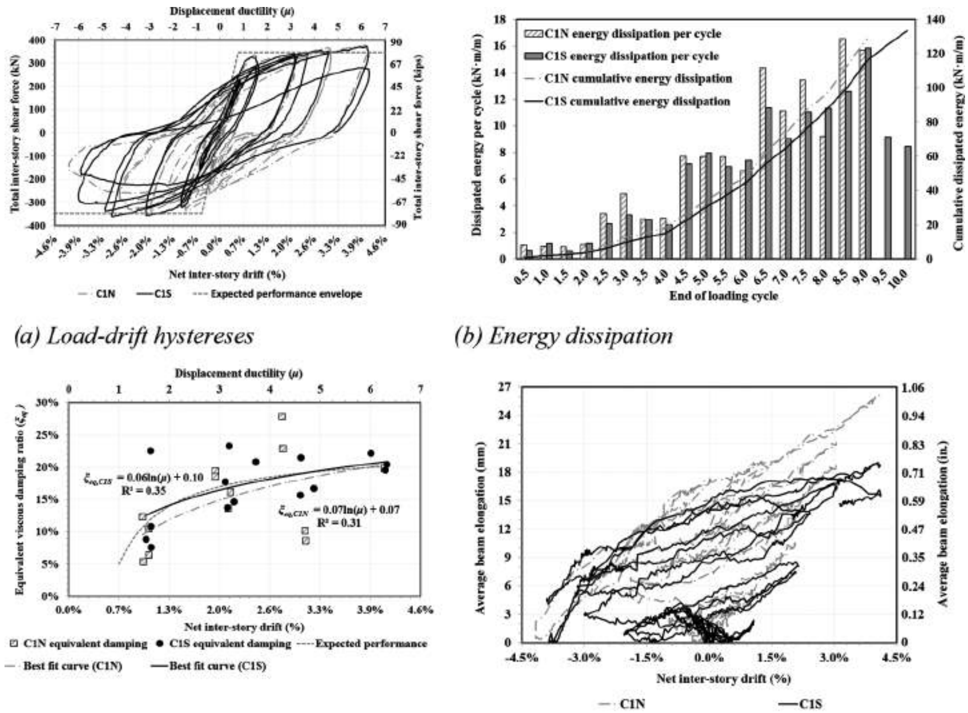

(a) Load-drift hystereses

(b) Energy dissipation

(c) Equivalent viscous damping

(d) Beam elongation

Fig. 12—Comparison of global performance of two cruciform test specimens. (Note: 1 kN = 0.225 kip.)

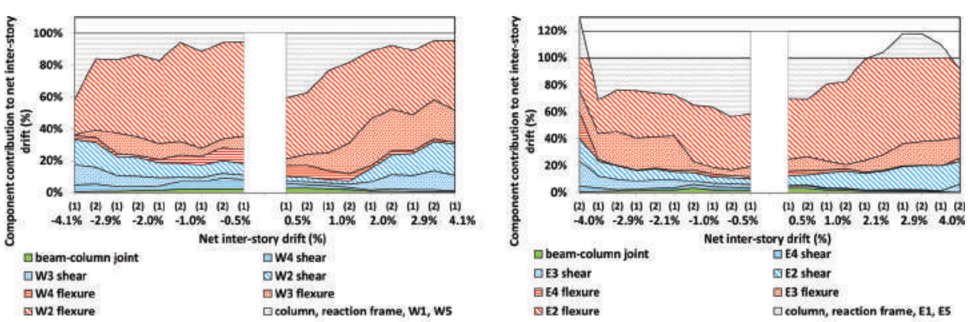

(a) C1N

(b) C1S

Fig. 13—Component contributions to interstory drifts of cruciform specimens.

of 0.65% and a nearly equivalent interstory shear strength were measured for both cruciform beams during testing (refer to Fig. 12(a));

3. Deformation and damage in the H-frame beams were due largely to the development of shear-sliding mechanisms located in the regions near the "bend" in the diagonal beam reinforcement (refer to Fig. 2(a), 8, and 10), as previously observed in testing of precast RC beams with similar reinforcement details[13,17] and predicted by analyzing these diagonal bar details using a strut-and-tie model[10,11];

4. Deformation and damage in the cruciform beams was due largely to the development of a flexural plastic hinge at the beam ends near the joint region, as is expected in typical moment-resisting RC frames[19];

5. Consistent with the improvements observed in previous testing of similar units,[13,17] the performance of Specimen H1 (having been both repaired and retrofitted with additional transverse steel reinforcement) exceeded the performance of Specimen H2 (having been repaired to its effectively as-built condition) in terms of strength, energy dissipation, and residual stiffness (refer to Fig. 9(a), 9(b), and 9(d), respectively). However, the retrofit technique used in Specimen H1 did not prevent shear-sliding mechanisms in gauge panel regions E1 and W1 from occurring (Fig. 8), contrary to the retrofit design intent; and

6. The equivalent damping capacity of the H-frame specimens (refer to Fig. 9(c)) was slightly less at high ductility demands than would be expected for more typically detailed RC frames, but the equivalent damping capacity of the precast RC cruciform beams (refer to Fig. 12(c)) was comparable to that expected in typically detailed RC frames.[19]

SUMMARY AND CONCLUSIONS

Three precast RC moment-frame specimens were extracted during the demolition of Clarendon Tower in Christchurch, New Zealand after sustaining damage during the 2010-2011 Canterbury earthquake sequence. These specimens were tested as part of a research program, with important implications for engineering researchers and consultants. By applying quasi-static, cyclic loading to the specimens using methods commonly used in New Zealand and internationally for testing moment-resisting frames, and comparing the performance to experimentally derived results and empirical predictive models from various research investigations around the world, the following conclusions were demonstrable:

1. The H-frame precast RC beams with "shear-ductile" detailing (refer to Fig. 2(a)) exhibited less displacement ductility capacity and equivalent viscous damping capacity than more conventionally detailed beams designed for flexural hinge formations (Fig. 2(b));

2. The non-retrofitted H-frame shear-ductile beam (Specimen H2) was determined to have sufficient strength and displacement capacity to meet its contemporary design demands (as proven by both the 2011 Christchurch earthquake as well as this deliberate experimental testing program), and it did not appear to be affected by low-cycle fatigue in the steel reinforcement;

3. The retrofitted H-frame shear-ductile beam (Specimen H1) was able to be repaired and retrofitted to an enhanced strength capacity without reducing the displacement capacity as compared to its non-retrofitted counterpart (Specimen H2); and

4. The conventionally detailed cruciform beams (refer to Fig. 2(b)) provided a high displacement ductility capacity and typical equivalent viscous damping capacity, validating the viability of the contemporary precast construction method used in Clarendon Tower for buildings in areas of moderate to high seismicity.

AUTHOR BIOS

Kevin Walsh *is a Structural Engineer at Frost Engineering and Consulting, Mishawaka, IN, and is a doctoral candidate at the University of Auckland, Auckland, New Zealand. His research interests include seismic design and assessment of buildings and seismic risk profiling of regional building stocks.*

ACI member **Richard Henry** *is a Lecturer in the Department of Civil and Environmental Engineering at the University of Auckland. His research interests include the seismic design of reinforced and prestressed concrete structures, precast concrete construction, and low-damage seismic design.*

Gye Simkin *is a Doctoral Candidate at the University of Auckland. His research interests include monitoring the seismic performance and damage of both new and existing concrete buildings using advanced sensor technologies.*

Nicholas Brooke *is a Structural Engineer at Compusoft Engineering Ltd., Auckland, New Zealand. He received his PhD in structural engineering from the University of Auckland.*

Barry Davidson *is Director at Compusoft Engineering Ltd. His research interests include analysis and design of most structural forms, including high-rise buildings, bridges, concrete arch dams, offshore gas platforms, and hyperbolic cooling towers.*

ACI member **Jason Ingham** *is a Professor of structural engineering at the University of Auckland. His research interests include seismic assessment and retrofit of masonry and concrete buildings.*

ACKNOWLEDGMENTS

The majority of the cost of the testing described in this paper was borne by Mitsui Sumitomo Insurance Group and their reinsurers. The permission granted to publish the results of the testing openly is greatly appreciated. Many parties contributed to the testing program, with particular acknowledgements due to the assistance provided by CAL Engineering Management, Contech, Auckland Cranes, and D&H Steel Construction. R. Leynaud from ENSTA ParisTech, and S. Corney and Y. Lu from the University of Auckland contributed to the instrumentation and testing efforts as well.

REFERENCES

1. Standards New Zealand (NZS), "3101 Part 1: Code of Practice for the Design of Concrete Structures," Wellington, New Zealand, 1982, 127 pp.

2. Standards New Zealand (NZS), "4203: Code of Practice for General Structural Design and Design Loadings for Buildings," Wellington, New Zealand, 1984, 108 pp.

3. Brooke, N., "Improving the Performance of Reinforced Concrete Beam-Column Joints Designed for Seismic Resistance," doctoral thesis, University of Auckland, Auckland, New Zealand, 2011, 508 pp.

4. Holmes Wood Poole and Johnstone Ltd, "Structural Drawings: Clarendon Project," Paynter Developments Limited, 1987.

5. Park, R., "A Perspective on the Seismic Design of Precast Concrete Structures," *PCI Journal*, V. 40, No. 3, 1995, pp. 40-60. doi: 10.15554/pcij.05011995.40.60

6. Bull, D., "Guidelines for the Use of Structural Precast Concrete in Buildings: Report of a Study Group of the New Zealand Concrete Society and the New Zealand National Society for Earthquake Engineering," Centre for Advanced Engineering, Christchurch, New Zealand, 1991, 143 pp., caenz.squarespace.com/s/Precast_Concrete.pdf

7. Restrepo, J.; Park, R.; and Buchanan, A., "Design of Connections of Earthquake Resisting Precast Reinforced Concrete Perimeter Frames," *PCI Journal*, V. 40, No. 5, 1995, pp. 68-80. doi: 10.15554/pcij.09011995.68.80

8. Bradley, B., "Site-Specific and Spatially-Distributed Ground-Motion Intensity Estimation in the 2010-2011 Canterbury Earthquakes," *Soil Dynamics and Earthquake Engineering*, V. 61-62, June-July 2014, pp. 83-91. doi: 10.1016/j.soildyn.2014.01.025

9. Cattanach, A., and Thompson, J., "The Clarendon Tower Deconstruction: Lessons Learnt on 1980s Building Performance," The New Zealand Concrete Industry Conference, Queenstown, New Zealand, 2013, pp. 1-24.

10. Cooper, M.; Carter, R.; and Fenwick, R., "Final Report: Volume 2: The Performance of Christchurch CBD Buildings," Canterbury Earthquakes Royal Commission, Christchurch, New Zealand, 2012, 237 pp., http://canterbury.royalcommission.govt.nz/Final-Report-Volume-Two-Contents

11. Zimmerman, R., and Holmes, W., "Seismic Performance Investigation: Clarendon Tower," Rutherford & Chekene, San Fransisco, CA, 2012, http://canterbury.royalcommission.govt.nz /documents-by-key/20120229.3475

12. Fleischman, R.; Restrepo, J.; Pampanin, S.; Maffei, J.; Seeber, K.; and Zahn, F., "Damage Evaluations of Precast Concrete Structures in the 2010-2011 Canterbury Earthquake Sequence," *Earthquake Spectra*, V. 30, No. 1, 2014, pp. 277-306. doi: 10.1193/031213EQS068M

13. Restrepo, J.; Park, R.; and Buchanan, A., "Tests on Connections of Earthquake Resisting Precast Reinforced Concrete Perimeter Frames of Buildings," *PCI Journal*, V. 40, No. 4, 1995, pp. 44-61. doi: 10.15554/pcij.07011995.44.61, https://www.pci.org/pci_journal-1995-july-august-5/

14. Park, R., "Evaluation of Ductility of Structures and Structural Assemblages from Laboratory Testing," *Bulletin Of The New Zealand National Society For Earthquake Engineering*, V. 22, No. 3, 1989, pp. 155-166, http://www.nzsee.org.nz/db/Bulletin/Archive/22(3)0155.pdf.

15. ACI Committee 374, "Guide for Testing Reinforced Concrete Structural Elements under Slowly Applied Simulated Seismic Loads (ACI 374.2R-13)," American Concrete Institute, Farmington Hills, MI, 2013, 18 pp.

16. ASCE, "Seismic Evaluation and Retrofit of Existing Buildings (ASCE 41-13)," American Society of Civil Engineers, Reston, VA, 2014, 518 pp.

17. Restrepo-Posada, J., "Seismic Behaviour of Connections between Precast Concrete Elements," doctoral thesis, University of Canterbury, Christchurch, New Zealand, 1993, http://hdl.handle.net/10092/7666

18. Priestley, M., "Brief Comments on Elastic Flexibility of Reinforced Concrete Frames and Significance to Seismic Design," *Bulletin of the New Zealand National Society for Earthquake Engineering*, V. 31, No. 4, 1998, pp. 246-259, http://www.nzsee.org.nz/db /Bulletin/Archive/31(4)0246.pdf.

19. Priestley, M.; Calvi, G.; and Kowalsky, M., *Displacement-Based Seismic Design of Structures*, IUSS Press, Pavia, Italy, 2007, 721 pp.

20. Standards New Zealand (NZS), "3112.2 Part 2: Tests Relating to the Determination of Strength of Concrete," 12th edition, Wellington, New Zealand, 1986, 22 pp.

21. ASTM C39/C39M-14, "Standard Test Method for Compressive Strength of Cylindrical Concrete Specimens," ASTM International, West Conshohocken, PA, 2011, 7 pp. doi: 10.1520/C0039_C0039M-14A10.1520/C0039_C0039M-14A

22. Restrepo-Posada, J.; Dodd, L.; Park, R.; and Cooke, N., "Variables Affecting Cyclic Behavior of Reinforcing Steel," *Journal of Structural Engineering*, ASCE, V. 120, No. 11, 1994, pp. 3178-3196. doi: 10.1061/(ASCE)0733-9445(1994)120:11(3178)

23. Mander, J.; Panthaki, F.; and Kasalanati, A., "Low-Cycle Fatigue Behavior of Reinforcing Steel," *Journal of Materials in Civil Engineering*, V. 6, No. 4, 1994, pp. 453-468. doi: 10.1061/(ASCE)0899-1561(1994)6:4(453)

24. "Clarendon Tower," 43.531395° S and 172.634025° E, Google Earth, 2014, http://www.google.com/earth/. (last accessed Mar. 21, 2014)